DOI 10.1002/bit.25212

The Role of Substrate Binding Pocket Residues Phenylalanine 176 and Phenylalanine 196 on *Pseudomonas* sp. OX1 Toluene *o*-Xylene Monooxygenase Activity and Regiospecificity†

Burcu Sönmez[1], Kübra Cansu Yanık-Yıldırım[1], Thomas K. Wood[2], Gönül Vardar-Schara[1*]

[1]Department of Genetics and Biongineering, Fatih University, Buyukcekmece, Istanbul 34500 TURKEY

[2]Department of Chemical Engineering and Department of Biochemistry and Molecular Biology, Pennsylvania State University, University Park, Pennsylvania, U.S.A.

***Corresponding author:** Phone: 90 (212) 866-3300 / 5644, Fax: 90 (212) 866-3412

Email: gschara@fatih.edu.tr

Short running title: The role of ToMO F176 and F196 on catalysis

Keywords: toluene-*o*-xylene monooxygenase, saturation mutagenesis, regiospecific oxidation

†This article has been accepted for publication and undergone full peer review but has not been through the copyediting, typesetting, pagination and proofreading process, which may lead to differences between this version and the Version of Record. Please cite this article as doi: [10.1002/bit.25212]

© 2014 Wiley Periodicals, Inc.
Received October 17, 2013; Revision Received December 27, 2013; Accepted February 6, 2014

Accepted Preprint

ABSTRACT

Saturation mutagenesis was used to generate eleven substitutions of toluene-*o*-xylene monooxygenase (ToMO) at alpha subunit (TouA) positions F176 and F196 among which nine were novel: F176H, F176N, F176S, F176T, F196A, F196L, F196T, F196Y, F196H, F196I, and F196V. By testing the substrates phenol, toluene, and naphthalene, these positions were found to influence ToMO oxidation activity and regiospecificity. Specifically, TouA variant F176H was identified that had 4.7-, 4.3-, and 1.8-fold faster hydroxylation activity towards phenol, toluene, and naphthalene, respectively compared to native ToMO. The F176H variant also produced the novel product hydroquinone (61%) from phenol, made 2-fold more 2-naphthol from naphthalene (34% versus 16% by the wild-type ToMO), and had the regiospecificity of toluene changed from 51% to 73% *p*-cresol. The TouA F176N variant had the most *para*-hydroxylation capability, forming *p*-cresol (92%) from toluene and hydroquinone (82%) from phenol as the major product, whereas native ToMO formed 30% *o*-cresol, 19% *m*-cresol, and 51% of *p*-cresol from toluene and 100% catechol from phenol. For naphthalene oxidation, TouA variant F176S exhibited the largest shift in the product distribution by producing 3-fold more 2-naphthol. Among the other F196 variants, F196L produced catechol from phenol 2-times faster than the wild-type enzyme. The TouA F196I variant produced 2-fold less *o*-cresol and 19% more *p*-cresol from toluene, and the TouA F196A variant produced 62% more 2-naphthol from naphthalene compared to wild-type ToMO. Both of these positions have never been studied through the saturation mutagenesis and some of the best substitutions uncovered here have never been predicted and characterized for aromatics hydroxylation.

Accepted Preprint

INTRODUCTION

The biocatalyst toluene-*o*-xylene monooxygenase (ToMO) of *Pseudomonas* sp. OX1 (Cafaro et al. 2002; Radice et al. 2006) belongs to a remarkable family of bacterial multicomponent monooxygenases (BMM) (Notomista et al. 2003) and has been shown to have a great potential for biotechnological and environmental applications (Notomista et al. 2011; Vardar et al. 2005a; Vardar et al. 2005b; Vardar and Wood 2004; Vardar and Wood 2005b).

Protein engineering is the process of creating altered forms of a known enzyme catalyst to increase its catalytic function, alter its substrate specificity or stereospecificity, and/or increase its stability (2009). There are two main approaches to protein engineering: rational design (Steiner and Schwab 2012) and directed evolution (Bloom and Arnold 2009; Goldsmith and Tawfik 2012; Turner 2009; Wang et al. 2012), which can be combined to semi-rational design (Bornscheuer and Kazlauskas 2011; Bornscheuer et al. 2012; Bornscheuer and Pohl 2001; Böttcher and Bornscheuer 2010). Semi-rational approach of saturation mutagenesis combines the advantages of rational design and directed evolution, where only the position of the mutation is chosen based on the prior biochemical and/or structural knowledge and then saturated with all 19 possible amino acid substitutions; hence, creating smaller and higher quality libraries with less effort (Chica et al. 2005; Lutz 2010; Siloto and Weselake 2012). It can provide much more comprehensive information than single substitutions performed by the rational design approach of site-specific mutagenesis as well as overcome the disadvantages of random mutagenesis (Wood 2008).

The hydrophobic alpha subunit residues I100, E103, A107, Q141, F176, M180, L192, F196, T201, Q204, and F205 form the active site substrate binding pocket (Figure 1) and are mostly conserved among their BMM family member (Sazinsky et al. 2006). Most of these pocket residues have been the subject of several protein engineering studies and shown to influence the catalytic activity and regiospecificity (Cafaro et al. 2005; Fishman et al. 2005; McClay et al. 2005; Notomista et al. 2009; Notomista et al. 2011; Pikus et al. 2000; Pikus et al. 1997; Rui et al. 2005; Steffan and McClay 2000; Vardar et al. 2005a; Vardar and Wood 2004; Vardar and Wood 2005a). We have also previously published a summary table showing the important roles of some of these residues on catalysis (Vardar et al. 2005b). Of these residues, F176 and F196 are especially noteworthy since these positions have not been extensively studied through saturation mutagenesis and there are only a few studies performed by rational design approach of site-directed mutagenesis.

Accepted Preprint

The alpha subunit of ToMO (TouA) F176 residue is located in the first hydrophobic cavity housing the diiron center and 4.3 Å away from both the gate residue I100 and the aromatic substrate channel (McCormick and Lippard 2011; Sazinsky et al. 2004) (according to the CAVER (Petřek et al. 2006) and PyMOL (DeLano 2002) calculations) (Figure 1). Its closest C-C distance from Fe_A and Fe_B is 8.8 Å and 8.6 Å away, respectively. Residue 176 of ToMO has been studied previously using site directed mutagenesis and found to allow ToMO to oxidize 2-phenylethanol for the production of *p*-tyrosol (Notomista et al. 2011). Based on a computational model, ToMO single variants F176I, F176L, and F176T and double variants E103G/F176 (I, L, T, A, S, V) were generated via site-directed mutagenesis (Notomista et al. 2009; Notomista et al. 2011). All of the variants were able to produce only tyrosol from 2-phenylethanol, leading to exclusively *para* hydroxylation. In addition, the double mutants also showed enhanced catalytic activity compared to wild-type ToMO, among which E103G/F176T had the highest k_{cat} value (13-fold increase). It was concluded that the regiospecific change was due to the mutations at position F176 and the rate was enhanced due to the additional mutation at E103G (Notomista et al. 2011). In a different study with ToMO, variants T201S/F176A and T201S/F176W was isolated via site directed mutagenesis with 100% retained and diminished activity for phenol oxidation, respectively (Song et al. 2011). The role of position 176 as an active residue in the related enzyme toluene-4-monooxygenase (T4MO) has also been studied via site directed mutagenesis by generating two variants, TmoA F176A and F176L (Steffan and McClay 2000). It was found that changing phenylalanine at position 176 to a smaller residue such as alanine abolished the T4MO activity completely toward toluene, TCE, and butadiene and changing it to leucine led to slightly increased activity (12%) for TCE and lowered the activity for toluene (3.9-fold) and butadiene (2.6-fold) oxidation (Steffan and McClay 2000).

The TouA F196 residue is also located in the first hydrophobic cavity and 5.8 Å away from the gate residue I100 and 3.4 Å from the substrate channel (McCormick and Lippard 2011; Sazinsky et al. 2004) (Figure 1). Its closest C-C distance from Fe_A and Fe_B is 8.0 Å and 7.0 Å away, respectively. It is also just one amino acid away from the iron ligand Q197 that makes up the catalytic center of the enzyme (McCormick and Lippard 2011). Because of this proximity, it was suggested that altering F196 could lead to changes in catalytic activity (Steffan and McClay 2000). In addition, position F196 moved around 2 Å closer to the active site upon binding of the regulatory protein in the T201A T4moHD structure, which was suggested to cause an increased rate of catalysis (Bailey et al. 2012). To our knowledge, the role of TouA F196 residue on ToMO activity has never

Accepted Preprint

been studied before. However, McClay et *al.* studied the analog of this residue on T4MO activity by using site-directed mutagenesis (McClay et al. 2005; Sazinsky 2004; Steffan and McClay 2000). Four different mutations were generated at site T4MO F196; F196I, F196L, F196Y, F196G. It was found that changing phenylalanine at position 196 to the smallest residue glycine inhibited the T4MO activity completely toward toluene, TCE, and butadiene, whereas variant F196L was 79%, 117%, and 31% as active towards these substrates, respectively, as compared to the wild-type (Sazinsky 2004; Steffan and McClay 2000). In a different study, same T4MO variant F196L was shown to impact the regiospecificity of indole oxidation by increasing the oxindole formation two fold (McClay et al. 2005). Among all, T4MO variant F196I exhibited the largest shift in the product distribution from toluene by producing 5-fold more *o*-cresol and 7.5-fold more benzyl alcohol (Sazinsky 2004).

In the present work, positions TouA F176 and F196 were subjected to saturation mutagenesis for the first time with the goals of investigating their role in catalysis and generating further improvements in ToMO activity and regiospecificity for the oxidation of phenol, toluene, and naphthalene. Saturation mutagenesis was performed to achieve a comprehensive study by exploring all the substitutions for these codons. Eleven variants were isolated, among which the best substitutions uncovered here have never been predicted through rational design approaches before. This study confirms the advantages of the semi-rational approach for protein engineering and expands the knowledge on the architecture of the ToMO active site and its relation to the regiospecific oxidation of aromatics.

MATERIALS AND METHODS

Escherichia coli TG1 (Sambrook et al. 2000) was utilized to host pBS(Kan)ToMO (Vardar and Wood 2004) and its variants which stably and constitutively expresses the *touABCDEF* genes. TG1 transformed with the plasmid constructs was routinely cultivated and the relative protein expressions of the *touA*, *touE*, and *touF* loci were evaluated using sodium dodecyl sulfate-polyacrylamide gel electrophoresis (SDS-PAGE), as described previously (Vardar and Wood 2004). Chemicals were from Merck (Darmstadt, Germany) and Sigma-Aldrich (Steinheim, Germany).

A gene library encoding all possible amino acids at TouA positions F176 and F196 was constructed by replacing the target codon with NNN via three-step overlap extension PCR as described previously (Vardar and Wood 2004). To perform saturation mutagenesis at TouA position F176, a 700 bp DNA fragment that includes the *Kpn*I restriction site upstream of codon F176 was amplified using primers ToMO-*Kpn*I-front and F176-rear,

Accepted Preprint

and a 957 bp DNA fragment that includes the *Sal*I restriction site downstream of codon F176 was amplified using primers F176-front and ToMO-*Sal*I-rear (Table I). Similarly, to perform saturation mutagenesis at TouA position F196, a 763 bp DNA fragment was amplified using primers ToMO-*Kpn*I-front and F196-rear, and a 898 bp DNA fragment was amplified using primers F196-front and ToMO-SalI-rear. The two degenerate PCR fragments were combined to obtain the full length products (1314 bp) with the ToMO-*Kpn*I-front and ToMO-SalI-rear primers and the products was cloned using *Kpn*I and *Sal*I. *Pfu Ultra II* high-fidelity polymerase (Stratagene, La Jolla, CA) was used to minimize random point mutations. Total of 850 colonies from both F176 and F196 libraries were screened on phenol using a rapid nylon membrane assay (Vardar and Wood 2004) to ensure that all of the 64 possible codons were sampled (Rui et al. 2004). To create the TouA F176H/F196L double mutant, site directed mutagenesis was performed to add F196L to TouA using the TouA F176H variant as a PCR template. A similar approach was used as described above using primers F196L-front and F196L-rear (Table I). The product formation rates and regiospecificity from substrates including 800 μM phenol, 250 μM toluene (91 μM based on Henry's Law constant of 0.27 (Dolfing et al. 1993)), and 5 mM naphthalene (solubility is 0.23 mM in water (Perry and Chilton 1973)) were determined after a contact period of 5 minutes to 2 hours as described previously (Vardar and Wood 2004) using reverse-phase high-performance liquid chromatography (HPLC, LC-20AT, Shimatzu, Japan) coupled to a diode array detector (SPD-M20A, Shimatzu, Japan) and an autosampler (SIL-20A, Shimatzu, Japan). When toluene was the substrate, an Astec CYCLOBOND I2000 column (Supelco Analytical, 25 cm x 4.6 mm, 5 μm) was used with an isocratic mobile phase of H_2O and methanol (80:20) at a flow rate of 1 mL/min. Under these conditions, the retention times for *o*-cresol, *m*-cresol, and *p*-cresol were 4.9, 5.5, and 7.7 minutes, respectively and the absorbance maxima were 270, 271, and 277, respectively. At least two replicates of both wild-type ToMO and ToMO variants were analyzed for each substrate, and at least five injections were made for each substrate.

DNA sequencing was performed using the dideoxy chain-termination technique (ElimsBio, CA) with the primers listed in Table I. The sequences were analyzed using the Vector NTI software (Invitrogen, USA). The Swiss-Pdb Viewer (Guex and Peitsch 1997) was utilized to perform amino acid substitutions isosterically at TouA F176 and F196 based on residue interactions, steric hindrance, and energy minimization. The coordination of the TouA variants were built by introducing substitutions in the wild-type ToMO (PDB code: 1T0Q (Sazinsky et al. 2004)) and the best rotomer was selected based on the criterion that the side chain

Accepted Preprint

conformation is at the lowest energy state. Figure 1 was prepared using the molecular visualization program PyMOL (DeLano 2002) and CAVER software (Petřek et al. 2006) was used as PyMOL plugin to visualize the channels. All the distance measurements and H-bond analysis were done using both PyMOL and Swiss-Pdb Viewer.

RESULTS

Saturation mutagenesis was performed individually at amino acid positions TouA F176 and F196 to fully study their role on ToMO catalytic activity and regiospecificity for phenol, toluene and naphthalene oxidation. Libraries of more than 3000 colonies were obtained and 850 colonies from both libraries were screened for increased and altered activity on phenol. Eleven mutants with possible enhanced or altered activity from the F176 library were selected after three rounds of screening, and sequencing revealed that four different enzymes were created (Table II). TouA variant F176H and F176T were selected five and four times, respectively. Seventeen mutants with possible altered activity from the F196 library were selected, and sequencing revealed that seven different enzymes were created (Table III). TouA variants F196Y, F196L, F196T, and F176A were selected four, five, three, and two times, respectively. Sequencing the cloned region indicated that no other amino acids were changed. Variant F176H was sequenced on two separate occasions due to its increased indigoid production and formation of a differently colored (dark brown) product compared to wild-type ToMO. The formation of the brown color was observed with all the other F176 variants but with less intensity. On the other hand, the F196 library contained more various shades of blue colored colonies than F176 library did, in addition to the original blue color of wild-type ToMO on LB media agar plates containing kanamycin.

Eleven variants initially identified by the nylon membrane assay were further characterized by HPLC and the data obtained for wild-type ToMO were in close agreement with our earlier studies (Vardar and Wood 2004; Vardar and Wood 2005b) (Tables II and III). For phenol oxidation, the TouA F176N and F176H variants caused a large shift in product distribution among all the other variants isolated here and formed primarily hydroquinone, whereas wild-type ToMO formed only catechol (Table II). In terms of activity, variant F176H was a better catalyst than wild-type ToMO, exhibiting a 5-fold higher total product formation rate. Note that the TouA F176N and TouA F176H substitutions have never been isolated and characterized for any substrates before. Oxidation of phenol by TouA variants F176S and F176T also yielded hydroquinone, however with a reduced rate compared to wild-type ToMO (2.7- and 3.6-fold, respectively). On the other hand, all the seven

Accepted Preprint

F196 variants exhibited similar regiospecificities to ToMO for phenol and TouA F196L variant showed slightly enhanced catechol formation rates (Table III). Interestingly, combining the two beneficial mutations (F176H and F196L) altered the regiospecificity further; however the activity gains were not additive (Table II).

For naphthalene oxidation, variant TouA F176S showed the most drastic change in regiospecificity among all the other variants by producing equal amounts of 1- and 2-naphthol, but at 57% of the wild-type ToMO total rate (Table II). There was also a 2.8-, 2.4-, and 2.1-fold change in regiospecificity for 2-naphthol formation with variant F176T, F176N and F176H, respectively. Most of the F196 variants exhibited similar regiospecificities to ToMO for naphthalene except for TouA F196I and F196A (Table III). Mutants F196I and F196A oxidized naphthalene to 21 and 25% 2-naphthol, values which are 1.3- and 1.6-fold higher than the 2-naphthol percentage obtained with wild-type ToMO. Combination of F176H/F176L was additive for naphthalene oxidation, affecting both regiospecificity as well as activity (Table II).

For the oxidation of the natural substrate toluene, all of the F176 variants showed significant preference for C-4 hydroxylation and yielded more *p*-cresol compared to wild-type ToMO (Table II). Variant TouA F176N caused the largest shift in *p*-cresol formation but at half the wild-type rate, whereas F176H exhibited a 4-fold higher total cresol formation rate. Among the F196 variants, TouA F196I, F196T, F196V variants resulted in elevated *p*-cresol formation at the expense of both *o*- and *m*-cresol formation, whereas TouA F196A variant resulted in slightly elevated *m*-cresol formation at the expense of *p*-cresol formation (Table III).

To confirm that the increase in the activity of the TouA variants F176H and F196L derived from the amino acid substitutions rather than increased enzyme expression levels, SDS-PAGE was used. The expression levels of the TouA variant F196L was approximately the same as that of wild-type ToMO, hence the increase in the activity appears to arise from the mutation and not from different expression levels. TouA variant F176H was an expression down mutant; a single amino acid change led to around 2-fold less enzyme expression levels compared to that of wild-type ToMO. Hence, the activity of variant F176H might be even 2-fold more than the rates shown in Table II.

DISCUSSION

It is clearly shown in this study that residues TouA F176 and F196 affect catalytic activity and/or regiospecificity towards phenol, toluene, and naphthalene. Phenylalanine residues at position 176 and 196 are conserved in all other related toluene monooxygenases (TMO) and mark the entrance to the active site cavity

Accepted Preprint

along with isoleucine residue at position 100 (Sazinsky et al. 2004) (Figure 1). Saturation mutagenesis was used in order to study these positions comprehensively and this approach enabled us to isolate beneficial substitutions which were not predicted by rational design approach of site-directed mutagenesis before. It is also worth noting that this saturation mutagenesis was previously shown to be beneficial and chosen as the preferred method to study some of the other substrate binding pocket residues of TMOs (Rui et al. 2004; Tao et al. 2004; Vardar et al. 2005a; Vardar and Wood 2004; Vardar and Wood 2005a; Vardar and Wood 2005b). Eleven substitutions were isolated, among which nine were novel in ToMO and eight among the related family enzymes. To our knowledge, there is no previous data indicating the role of TouA position F196 on ToMO activity and regiospecificity. In addition, both TouA positions F176 and F196 have never been studied through the saturation mutagenesis approach for the hydroxylation of aromatics.

Using site directed mutagenesis, Notomista et *al.* previously studied two of the substitutions isolated here, F176T and F176S, for the oxidation of tyrosol, and these changes resulted in preference for *para*-hydroxylation in ToMO (Notomista et al. 2011). In addition, Notomista et *al.* successfully predicted that variants TouA F176I and F176L would have better *para* acting properties for toluene and *o*-xylene oxidation by computational modeling (Notomista et al. 2009). Here, we report that all of our F176 variants also acted like a *para* enzyme, correlating well with the previous work. For naphthalene oxidation, we observed that mutations which reduce the volume of the residue 176 increased the percentage of 2-naphthol production, agreeing well with the previously reported computational model prediction (Notomista et al. 2009). For example, phenylalanine with the largest volume among all made 16% 2-naphthol, whereas serine with the smallest volume made 50% (Table II). As the volume of the residue in the position decreased (phenylalanine, histidine, asparagine, threonine, and serine), the percentage of 2-naphthol production increased (16, 34, 39, 44, and 50%, respectively).

Using site directed mutagenesis, three of the substitutions isolated here, F196L, F196I, and F196Y, have been studied before for the oxidation of indole, toluene, TCE, and/or butadiene in the related enzyme T4MO (McClay et al. 2005; Sazinsky 2004; Steffan and McClay 2000). It was found that changing phenylalanine to leucine resulted in appreciable change in the product distribution for the oxidation of indole with 74% activity as compared to wild-type T4MO (McClay et al. 2005). In a different study, the same substitution in T4MO led to slightly increased activity for TCE (1.2-fold) and lowered activity for toluene (1.3-fold) and butadiene (3.3-fold) oxidation (Steffan and McClay 2000). Here, we report that L196 of ToMO TouA also had slightly

Accepted Preprint

enhanced activity toward phenol (2-fold). Furthermore, we observed that TouA F196 saturation mutagenesis library contained colonies with several ranges of indigo color, suggesting that ToMO TouA F196 might be also important for the regiospecificity of indole oxidation. These results are in accord with the previous studies with TmoA F196 described above. For toluene regiospecificity, substitution of isoleucine for phenylalanine 196 in T4MO caused the most impact, whereas substitutions of tyrosine resulted in no major changes in the product distribution (Sazinsky 2004). Similarly, we found that substitutions of isoleucine for phenylalanine 196 in ToMO led to the most dramatic change in the regiospecific hydroxylation of toluene among all the ToMO F196 variants, however with an adverse effect. Unlike TmoA F196I, variant TouA F196I exhibited higher *para* hydroxylating capability (Table III). Similar to TmoA F196Y, variant TouA F196Y also gave no change in the regiospecificity of toluene, as well as phenol and naphthalene. The effect of the mutations at F196 as well as at F176 may be substrate-dependent and work may be extended to study oxidation of other substrates in the future.

The modeling of the side chains of variants TouA F176 and F196 (Figure 1) suggests that substitutions at these positions may result in changes in the topology of the substrate binding cavity and may also alter the distances of the side chains with respect to iron atoms, gate residue (I100), channel residues (Q204), and other substrate binding pocket residues (E103). Recent structure-mechanism as well as modeling studies provide valuable insights for substrate docking at the active site pocket (Bailey et al. 2012; McCormick and Lippard 2011; Notomista et al. 2009). For all of the F176 variants, the changes in the reduced size of the side chain of residue 176, which expands the active site pocket and might have caused the benzene ring of toluene to shift such that the C-4 is directed more towards the diiron center. Similar considerations may apply to the *para*-hydroxylation capability of all the F176 variants for phenol oxidation. Furthermore, TouA mutations F176T, F176S and F176N may introduce additional H-bonds with the side-chain of E103, whereas F176H does not cause any H-bond formation with its neighbors (Figure 1). On the other hand, F176H substitution contains an imidazole functional group which is most likely deprotonated inside the hydrophobic pocket, behaving like a slightly larger version of asparagine. This may explain why F176H and F176N substitutions share similar characteristics like the ability to produce large amounts of novel product hydroquinone (Table II). It was previously shown that the F176W substitution contracted the entrance to cavity 1, abolishing phenol oxidation activity of ToMO (Song et al. 2011). While insertion of a smaller residue alanine at position 176 abolished the

Accepted Preprint

activity of T4MO (Steffan and McClay 2000), ToMO remained active (Song et al. 2011). Here, we observed that the residue in position F176 does not need to be hydrophobic for ToMO to be efficient catalysts and a small side chain is not a prerequisite. In addition, the substitution of phenylalanine, the most hydrophobic residue to asparagine, the most hydrophilic among all yielded the most *para*-acting properties (Table II).

Among the F196 variants, the side chain direction shifts with the F196I (Figure 1), F196V, and F196T substitutions, which may change the location of the methyl group of toluene to promote *p*-cresol formation by oxidation of the C-4. The shift was more with F196I compared to F196V and F196T, which may be the reason for the increase in *p*-cresol formation (Table III). Among all, only TouA mutation F196T may introduce a hydrogen bond with the side chain of residue S265. It is interesting that although isoleucine and leucine have the same molecular weight and hydrophobicity, the leucine substitution caused the variant to have slightly enhanced activity for phenol, whereas isoleucine had lowered activity; hence this shows a change in enzyme activity due to an amino acid substitution that does not alter the residue size and hydrophobicity. In general, TouA F196 can accommodate either hydrophobic or hydrophilic substitutions and most remained active for the oxidation of the tested substrates.

This study adds to the list of research in which substituting a single amino acid for another one can alter regiospecificity and enhance activity of ToMO. For example, we have previously shown that substituting glutamic acid at TouA position 214 located at the entrance of the substrate tunnel with glycine or isoleucine at TouA position 100 located at the entrance to the active site pocket with glutamate improved the oxidation activity (Vardar and Wood 2005a; Vardar and Wood 2005b). Our initial data indicates that combination of E214G with I100Q appeared to be substrate dependent and enhance the oxidation activity further (data not shown). Our results in this study also show that combination of F176H with F196L mutation affects the regiospecificity as well as activity of ToMO. It would be interesting to examine the effect of combining different beneficial mutations and extend the work to other substrates to improve the versatility of this remarkable enzyme.

ACKNOWLEDGEMENTS

This study was supported by the Marie Curie European Reintegration grant (PIRG07-GA-2010-268201). Conflict of interests: None declared.

Accepted Preprint

REFERENCES

Bailey LJ, Acheson JF, McCoy JG, Elsen NL, Phillips Jr GN, Fox BG. 2012. Crystallographic analysis of active site contributions to regiospecificity in the diiron enzyme toluene 4-monooxygenase. Biochemistry 51:1101-1113.

Bloom JD, Arnold FH. 2009. In the light of directed evolution: pathways of adaptive protein evolution. Proc Natl Acad Sci U S A 106:Suppl 1:9995-10000.

Bornscheuer U, Kazlauskas RJ. 2011. Survey of protein engineering strategies. Curr Protoc Protein Sci 66:26.7.1-26.7.14.

Bornscheuer UT, Huisman GW, Kazlauskas RJ, Lutz S, Moore JC, Robins K. 2012. Engineering the third wave of biocatalysis. Nature 485:185-194.

Bornscheuer UT, Pohl M. 2001. Improved biocatalysts by directed evolution and rational protein design. Curr Opin Chem Biol 5:137-143.

Böttcher D, Bornscheuer UT. 2010. Protein engineering of microbial enzymes. Curr Opin Microbiol 13:274-282.

Cafaro V, Notomista E, Capasso P, Donato AD. 2005. Mutation of glutamic acid 103 of toluene *o*-xylene monooxygenase as a means to control the catabolic efficiency of a recombinant upper pathway for degradation of methylated aromatic compounds. Appl Environ Microbiol 71:4744-4750.

Cafaro V, Scognamiglio R, Viggiani A, Izzo V, Passaro I, Notomista E, Piaz FD, Amoresano A, Casbarra A, Pucci P and others. 2002. Expression and purification of the recombinant subunits of toluene/*o*-xylene monooxygenase and reconstitution of the active complex. Eur J Biochem 269:5689-5699.

Chica RA, Doucet N, Pelletier JN. 2005. Semi-rational approaches to engineering enzyme activity: combining the benefits of directed evolution and rational design. Curr Opin Biotechnol 16:378-384.

DeLano WL. 2002. The PyMOL Molecular Graphics System San Carlos, CA, USA: DeLano Scientific.

Dolfing J, Wijngaard AJvd, Janssen DB. 1993. Microbiological aspects of the removal of chlorinated hydrocarbons from air. Biodegradation 4:261-282.

Fishman A, Tao Y, Rui L, Wood TK. 2005. Controlling the regiospecific oxidation of aromatics via active site engineering of toluene *para*-monooxygenase of *Ralstonia pickettii* PKO1. J Biol Chem 280:506-514.

Accepted Preprint

Goldsmith M, Tawfik DS. 2012. Directed enzyme evolution: beyond the low-hanging fruit. Curr Opin Struct Biol 22:406-412.

Guex N, Peitsch MC. 1997. SWISS-MODEL and the Swiss-PdbViewer: an environment for comparative protein modeling. Electrophoresis 18:2714-2723.

Lutz S. 2010. Beyond directed evolution--semi-rational protein engineering and design. Curr Opin Biotechnol 21:734-743.

Lutz S, Bornscheuer UT. 2009. Protein Engineering Handbook. Weinheim: WILEY-VCH Verlag GmbH & Co. KGaA.

McClay K, Boss C, Keresztes I, Steffan RJ. 2005. Mutations of toluene-4-monooxygenase that alter regiospecificity of indole oxidation and lead to production of novel indigoid pigments. Appl Environ Microbiol 71:5476-5483.

McCormick MS, Lippard SJ. 2011. Analysis of substrate access to active sites in bacterial multicomponent monooxygenase hydroxylases: X-ray crystal structure of xenon-pressurized phenol hydroxylase from *Pseudomonas* sp. OX1. Biochemistry 50:11058-11069.

Notomista E, Cafaro V, Bozza G, Donato AD. 2009. Molecular determinants of the regioselectivity of toluene/*o*-xylene monooxygenase from *Pseudomonas* sp. strain OX1. Appl Environ Microbiol 75:823-836.

Notomista E, Lahm A, Donato AD, Tramontano A. 2003. Evolution of bacterial and archaeal multicomponent monooxygenases. J Mol Evol 56:435-445.

Notomista E, Scognamiglio R, Troncone L, Donadio G, Pezzella A, Donato AD, Izzo V. 2011. Tuning the specificity of the recombinant multicomponent toluene *o*-xylene monooxygenase from *Pseudomonas* sp. strain OX1 for the biosynthesis of tyrosol from 2-phenylethanol. Appl Environ Microbiol 77:5428-5437.

Perry RH, Chilton CH. 1973. Chemical engineers' handbook. New York: McGraw-Hill.

Petřek M, Otyepka M, Banáš P, Košinová P, Koča J, Damborský J. 2006. CAVER: a new tool to explore routes from protein clefts, pockets and cavities. BMC Bioinformatics 7:1-9.

Pikus JD, Mitchell KH, Studts JM, McClay K, Steffan RJ, Fox BG. 2000. Threonine 201 in the diiron enzyme toluene 4-monooxygenase is not required for catalysis. Biochemistry 39:791-799.

Accepted Preprint

Pikus JD, Studts JM, McClay K, Steffan RJ, Fox BG. 1997. Changes in the regiospecificity of aromatic hydroxylation produced by active site engineering in the diiron enzyme toluene 4-monooxygenase. Biochemistry 36:9283-9289.

Radice F, Orlandi V, Massa V, Cavalca L, Demarta A, Wood TK, Barbieri P. 2006. Genotypic characterization and phylogenetic relations of *Pseudomonas* sp. (Formerly *P. stutzeri*) OX1. Curr Microbiol 52:395-399.

Rui L, Kwon YM, Fishman A, Reardon KF, Wood TK. 2004. Saturation mutagenesis of toluene *ortho*-monooxygenase of *Burkholderia cepacia* G4 for enhanced 1-naphthol synthesis and chloroform degradation. Appl Environ Microbiol 70:3246-3252.

Rui L, Reardon KF, Wood TK. 2005. Protein engineering of toluene *ortho*-monooxygenase of *Burkholderia cepacia* G4 for regiospecific hydroxylation of indole to form various indigoid compounds. Appl Microbiol Biotechnol 66:422-429.

Sambrook J, Russell D, Russell DW. 2000. Molecular cloning: a laboratory manual. New York: Cold Spring Harbor Laboratory Press. 2368 p.

Sazinsky MH. 2004. Structural studies of bacterial multicomponent monooxygenases: insights into substrate specificity, diiron center tuning and component interactions. Massachusetts Institute of Technology

Sazinsky MH, Bard J, Donato AD, Lippard SJ. 2004. Crystal structure of the toluene/*o*-xylene monooxygenase hydroxylase from *Pseudomonas stutzeri* OX1. Insight into the substrate specificity, substrate channeling, and active site tuning of multicomponent monooxygenases. J Biol Chem 279:30600-30610.

Sazinsky MH, Dunten PW, McCormick MS, DiDonato A, Lippard SJ. 2006. X-ray structure of a hydroxylase-regulatory protein complex from a hydrocarbon-oxidizing multicomponent monooxygenase, *Pseudomonas* sp. OX1 phenol hydroxylase. Biochemistry 45:15392-15404.

Siloto RMP, Weselake RJ. 2012. Site saturation mutagenesis: Methods and applications in protein engineering. Biocatal Agric Biotechnol 1:181-189.

Song WJ, Gucinski G, Sazinsky MH, Lippard SJ. 2011. Tracking a defined route for O_2 migration in a dioxygen-activating diiron enzyme. Proc Natl Acad Sci U S A 108:14795-14800.

Steffan RJ, McClay KR; 2000. Preparation of enantio-specific epoxides. United States of America.

Steiner K, Schwab H. 2012. Recent advances in rational approaches for enzyme engineering Comput Struct Biotechnol J 2(3):e201209010. doi: http://dx.doi.org/10.5936/csbj.201209010.

Accepted Preprint

Tao Y, Fishman A, Bentley WE, Wood TK. 2004. Altering toluene 4-monooxygenase by active-site engineering for the synthesis of 3-methoxycatechol, methoxyhydroquinone, and methylhydroquinone J Bacteriol 186:4705-4713.

Turner NJ. 2009. Directed evolution drives the next generation of biocatalysts. Nat Chem Biol 5:567-573.

Vardar G, Ryu K, Wood TK. 2005a. Protein engineering of toluene-*o*-xylene monooxygenase from *Pseudomonas stutzeri* OX1 for oxidizing nitrobenzene to 3-nitrocatechol, 4-nitrocatechol, and nitrohydroquinone. J Biotechnol 115:145-156.

Vardar G, Tao Y, Lee J, Wood TK. 2005b. Alanine 101 and alanine 110 of the alpha subunit of *Pseudomonas stutzeri* OX1 toluene-*o*-xylene monooxygenase influence the regiospecific oxidation of aromatics. Biotechnol Bioeng 92:652-658.

Vardar G, Wood TK. 2004. Protein engineering of toluene-*o*-xylene monooxyganase from *Pseudomonas stutzeri* OX1 for synthesizing 4-methylresorcinol, methylhydroquinone, and pyrogallol. Appl Environ Microbiol 70:3253-3262.

Vardar G, Wood TK. 2005a. Alpha-subunit positions methionine 180 and glutamate 214 of *Pseudomonas stutzeri* OX1 toluene-*o*-xylene monooxygenase influence catalysis. J Bacteriol 187:1511-1514.

Vardar G, Wood TK. 2005b. Protein enginering of toluene-*o*-xylene monooxygenase from *Pseudomonas stutzer*i OX1 for enhanced chlorinated ethene degradation and *o*-xylene oxidation. Appl Microbiol Biotechnol 68:510-517.

Wang M, Si T, Zhao H. 2012. Biocatalyst development by directed evolution. Biores Technol 115:117-125.

Wood TK. 2008. Molecular approaches in bioremediation. Curr Opin Biotechnol 19:572-578.

Accepted Preprint

Table I. Primers used for saturation mutagenesis of TouA F176 and F196, site-directed mutagenesis of TouA F176H/F196L, and sequencing the F176 and F196 region of the *touA* gene in TG1/pBS(Kan)ToMO.

Primer	Nucleotide sequence
Mutagenesis	
ToMO-*Kpn*I-front	5'-CCGGCTCGTATGTTGTGTGGAATTGTGAGCGG-3'
ToMO-*Sal*I-rear	5'-CCCACTCATAATCATGAGCGTCG-3'
F176-rear	5'-GGTCATCATCATGTCGTCNNNGAAAGACCGTGCAGCGATTG-3'
F176-front	5'-CAATCGCTGCACGGTCTTTCNNNGACGACATGATGATGACC-3'
F196-rear	5'-GCATATTGGTGAAGCCTGTTTCNNNTGCGAAGGTCAGCATGATAGAG-3'
F196-front	5'-CTCTATCATGCTGACCTTCGCANNNGAAACAGGCTTCACCAATATGC-3'
F196L-front	5'-CATGCTGACCTTCGCATTGGAAACAGGCTTCACC-3'
F196L-rear	5'-GGTGAAGCCTGTTTCCAATGCGAAGGTCAGCATG-3'
Sequencing	
F176_check_r	5'-GCGGCCAAACCGAGAAANNNCATATTGGTGAAGCCTGTTTCG-3'
F176_check_f	5'-CGAAACAGGCTTCACCAATATGNNNTTTCTCGGTTTGGCCGC-3'
F196_check_r	5'-CCGGTGAGTACCGANNNAAGCTTCCAAGATCGCCAGATTGCG-3'
F196_check_f	5'-GCAACTTCACTTCGGAGCGCAGGCACTTGAAGAATACGCCG-3'

Accepted Preprint

Table II. Oxidation of phenol, naphthalene, and toluene by *E. coli* TG1/pBS(Kan)ToMO expressing wild-type ToMO, saturation mutagenesis TouA F176 variants, and double variant F176H/F196L.

Enzyme	Phenol[a] oxidation			Naphthalene[a] oxidation			Toluene[a] oxidation			
	Regiospecificity (%)		Total product formation rate[b]	Regiospecificity (%)		Total product formation rate[b]	Regiospecificity (%)			Total product formation rate[b]
	Catechol	Hydroquinone		1-Naphthol	2-Naphthol		*o*-Cresol	*m*-Cresol	*p*-Cresol	
Wild-type	100	0	1.17 ± 0.42	84	16	0.47 ± 0.12	30	19	51	0.89 ± 0.12
F176H	39	61	5.53 ± 1.35	66	34	0.86 ± 0.22	12	15	73	3.80 ± 0.90
F176N	18	82	1.12 ± 0.81	61	39	0.42 ± 0.05	3	5	92	0.48 ± 0.16
F176S	85	15	0.43 ± 0.10	50	50	0.27 ± 0.01	4	7	89	1.64 ± 0.55
F176T	75	25	0.32 ± 0.10	56	44	0.17 ± 0.03	6	10	84	0.84 ± 0.17
F176H/ F196L	27	73	4.28 ± 0.23	77	23	0.54 ± 0.04	nm[c]	nm	nm	nm

[a]Initial concentration was 0.8 mM phenol, 0.23 mM naphthalene, and 91 µM toluene.
[b]Initial total product formation rate determined by HPLC in nmol/min/mg protein.
[c]nm, not measured

Accepted Preprint

Table III. Oxidation of phenol, naphthalene, and toluene by *E. coli* TG1/pBS(Kan)ToMO expressing wild-type ToMO and saturation mutagenesis TouA F196 variants.

[a]Initial concentration was 0.8 mM phenol, 0.23 mM naphthalene, and 91 μM toluene.

Enzyme	Phenol[a] oxidation		Naphthalene[b] oxidation			Toluene[c] oxidation			
	Regiospecificity (%)	Total product formation rate[b]	Regiospecificity (%)		Total product formation rate[b]	Regiospecificity (%)			Total product formation rate[b]
	Catechol		1-Naphthol	2-Naphthol		*o*-Cresol	*m*-Cresol	*p*-Cresol	
Wild-type	100	1.17 ± 0.42	84	16	0.47 ± 0.12	30	19	51	0.89 ± 0.12
F196A	100	1.18 ± 0.11	74	26	0.31 ± 0.01	29	25	46	1.27 ± 0.09
F196L	100	2.53 ± 0.56	86	14	0.48 ± 0.03	24	20	56	0.44 ± 0.18
F196T	100	1.92 ± 0.42	82	18	0.14 ± 0.01	24	15	61	0.92 ± 0.01
F196Y	100	1.22 ± 0.10	84	16	0.13 ± 0.01	29	19	52	0.34 ± 0.05
F196H	100	0.88 ± 0.11	86	14	0.12 ± 0.01	30	22	48	0.85 ± 0.02
F196I	100	0.81 ± 0.18	79	21	0.13 ± 0.01	14	16	70	0.21 ± 0.02
F196V	100	0.35 ± 0.01	84	16	0.04 ± 0.01	23	16	61	0.06 ± 0.01

[b]Initial total product formation rate determined by HPLC in nmol/min/mg protein.

Accepted Preprint

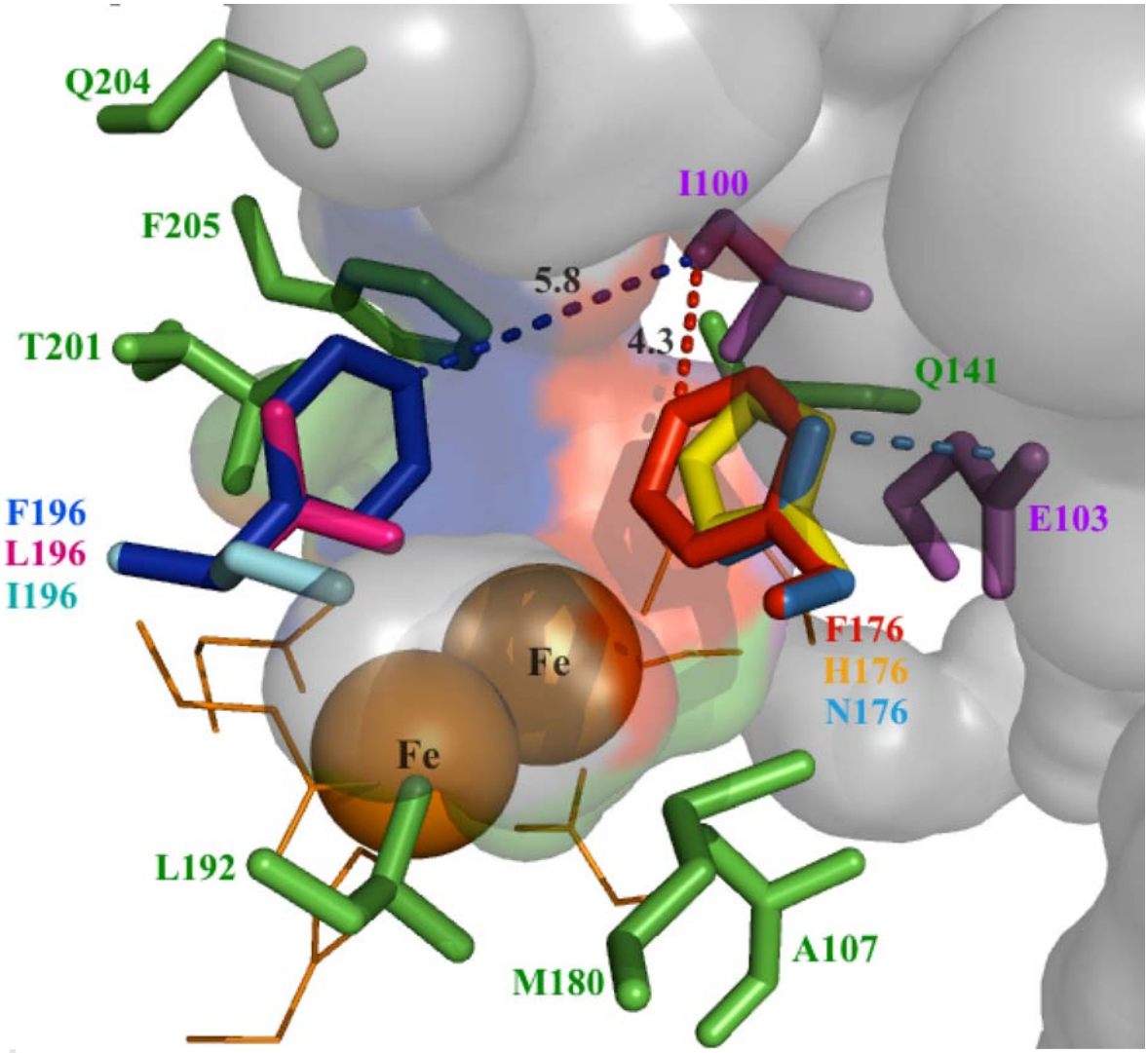

Figure 1

Active site pocket of the TouA alpha subunit of ToMO (PDB code: 1T0Q) showing the side chains of F176 (red) and F196 (blue) of the native ToMO along with TouA variants F176H (yellow), F176N (light blue), F196L (pink), and F196I (cyan). Residues in green (A107, Q141, M180, L192, T201, Q204, F205) and purple (I100, E103) are the side chains of the other substrate binding residues. Residues E104, E134, H137, E197, E231, and H234 (orange lines) coordinately bind to the iron atoms (orange spheres). Closest C-C distance (expressed in angstroms) of the I100 side group to the F176 and F196 is presented in a dashed red and blue line, respectively. The side chain of residue E103 participates in the new hydrogen bond (light blue dashed line) with the mutated residue N176. The surface of the cavities and pockets (culled) detected by PyMOL are shown in gray.

Accepted Preprint